Gabion Stepped Spillway: Interactions between Free-Surface, Cavity, and Seepage Flows

Gangfu Zhang[1] and Hubert Chanson[2]

Abstract: On a gabion stepped chute, the steps contribute to the dissipation of turbulent kinetic energy, free-surface aeration may be intense, and there are complex interactions between the free-surface flow and seepage motion. Detailed measurements were conducted in a relatively large gabion stepped spillway model. Using a combination of high-speed movies and phase-detection probe measurements, the air–water flow properties in the step cavities and in the gabions were documented. Strong air–water exchanges between seepage and stepped cavity flows were observed. The data showed a complex bubbly seepage motion in the gabions associated with a high level of interactions between seepage and free-surface flows, leading to a modification of the step cavity recirculation and lesser flow resistance. **DOI: 10.1061/(ASCE)HY.1943-7900.0001120.**

Author keywords: Air–water flow; Gabion stepped spillways; Seepage flow; Overflow-seepage flow interactions; Physical modeling.

Introduction

Stepped spillways have been used as flood release facilities for several centuries (Chanson 2001). The steps contribute to some dissipation of the turbulent kinetic energy, thereby reducing or eliminating the need for a downstream stilling structure. Highly turbulent flows are experienced down a stepped chute (Rajaratnam 1990). For low- to medium-head stepped chutes, gabions may be a suitable construction material. Their advantages include stability, low cost, flexibility, porosity, and noise abatement (Agostini et al. 1987; Chanson 2001). Peyras et al. (1992) investigated the flow patterns and energy dissipation performances of gabion stepped weirs with a 0.2 m step height. Wüthrich and Chanson (2014) compared the energy dissipation performances of flat impervious and gabion stepped chutes. Their findings showed lesser rates of energy dissipation on the gabion chutes, which motivated the present investigation.

Herein the turbulent flow properties above a gabion stepped chute were investigated experimentally. The air–water flow was studied in the mainstream flow and step cavities and within the gabions using a combination of dual-tip phase-detection probe and high-speed video observations. It is the aim of this study to detail the interactions between air–water seepage and cavity flows and to characterize the flow through gabions.

Experimental Setup and Instrumentation

Experiments were conducted at the University of Queensland in a gabion stepped chute, previously used by Wüthrich and Chanson (2014). The test section was 3 m long and 0.52 m wide, consisting of an impervious broad crest followed by ten 0.1 m high, 0.2 m long gabion steps: the chute slope was $\theta = 26.6°$ (1V:2H). Each gabion was 0.3 m long, 0.1 m high, and 0.52 m wide, filled with 14 mm sieved gravel, and the gabions overlapped (Fig. 1). The bulk density of the dry gravel was 1.6 t/m^3 with a porosity of approximately 0.35–0.4. The hydraulic conductivity of the gabions ranged from 1.1×10^{-1} to 2.3×10^{-1} m/s. The discharge was recorded from the upstream head above the crest. The air–water flow measurements were performed with a dual-tip phase-detection probe ($\emptyset = 0.25$ mm) in the free-surface flow and step cavities, with the probe sensors sampled at 20 kHz for 45 s. The translation of the probe in the normal direction was controlled by a fine adjustment traverse. Visual observations were made with high-speed video recordings at speeds of up to 1,000 fps (fps = frames per second).

The flow investigations were conducted for discharges per unit width up to 0.28 m^2/s, with a focus on the aerated transition and skimming flows, i.e., $d_c/h > 0.6$, where d_c is the critical flow depth [$d_c = (q^2/g)^{1/3}$], q is the discharge per unit width, g is the gravity acceleration, and h is the vertical step height. Phase-detection probe measurements were performed in the overflow including in the step cavities. Bubble trajectories in the gabions were tracked with the high-speed video camera. The tracking was performed using a manual frame-by-frame analysis to guarantee the maximum reliability of the data.

Flow Patterns

On the gabion stepped spillway, the water seeped through the gabions at very low discharges ($d_c/h < 0.2$), and no overflow was observed at the step edges. For $d_c/h > 0.2$, some overflow was observed above all the gabion steps. A nappe flow regime occurred for $0.2 < d_c/h < 0.5 - 0.6$. A transition flow was seen for $0.6 < d_c/h < 0.9$, characterized by large hydrodynamic instabilities and intense splashes in the overflow. For $d_c/h > 0$, a skimming flow was seen. The upstream flow was nonaerated. The inception of free-surface aeration was clearly marked. Downstream, the air-entrainment process was highly three-dimensional and complex.

The gabions were fully saturated for $d_c/h > 0.2$. Downstream of the inception point, a strong bubbly motion was observed inside all gabions, as sketched in Fig. 1. A large amount of air entered the gabions through the downstream half of the horizontal step face. The entrapped air flowed through the gabions as individual bubbles

[1]Ph.D. Research Student, School of Civil Engineering, Univ. of Queensland, Brisbane, QLD 4072, Australia.

[2]Professor in Hydraulic Engineering, School of Civil Engineering, Univ. of Queensland, Brisbane, QLD 4072, Australia (corresponding author). E-mail: h.chanson@uq.edu.au

Note. This manuscript was submitted on April 15, 2015; approved on October 20, 2015; published online on January 8, 2016. Discussion period open until June 8, 2016; separate discussions must be submitted for individual papers. This technical note is part of the ***Journal of Hydraulic Engineering***, © ASCE, ISSN 0733-9429.

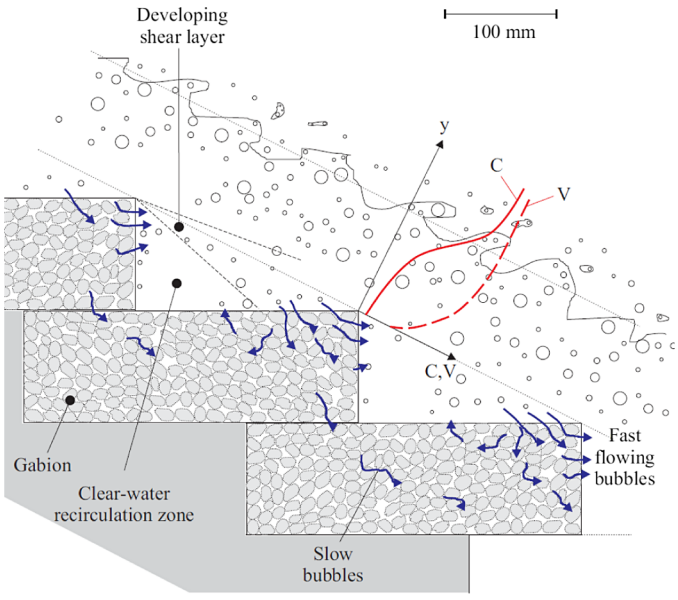

Fig. 1. Sketch of air–water flow patterns above a gabion stepped spillway: bubbly seepage motion, shown by arrows, and air–water free-surface flow above

and groups of bubbles. Fast flowing bubbles exited the gabions through the next vertical step face (Fig. 1). Other bubbles flowed downward before traveling back into the step cavity. More bubbles were entrained through the next gabion box. The bubbly seepage pattern and cavity flow motion suggested the existence of large positive pressures on the downstream end of the horizontal step faces and negative pressures on the upper part of the vertical step faces, in a manner consistent with the pressure data of Sánchez-Juny et al. (2007). In the gabion material, bubble recirculation, breakup, and coalescence took place. These processes were linked to the combination of constrictions between adjacent pieces of gravel as well as relatively large cavities between pebbles. The observations indicated a broad variety of bubble shapes, ranging from highly distorted and elongated shapes in regions of high shear to pseudo-ellipsoidal shapes in larger cavities.

Energetic air–water interactions were observed between the seepage and free-surface flows, next to the gabion step surfaces, and in the step cavity. The seepage appeared to modify the cavity recirculation pattern, compared to smooth impervious stepped chutes. A vertical flux of air bubbles was observed close to the vertical step face. Most bubbles came out of the gabion materials and were entrained upward in the cavity. In a third of the step cavity, a clear water core was seen, as illustrated in Fig. 1. This has never been reported on smooth impervious steps.

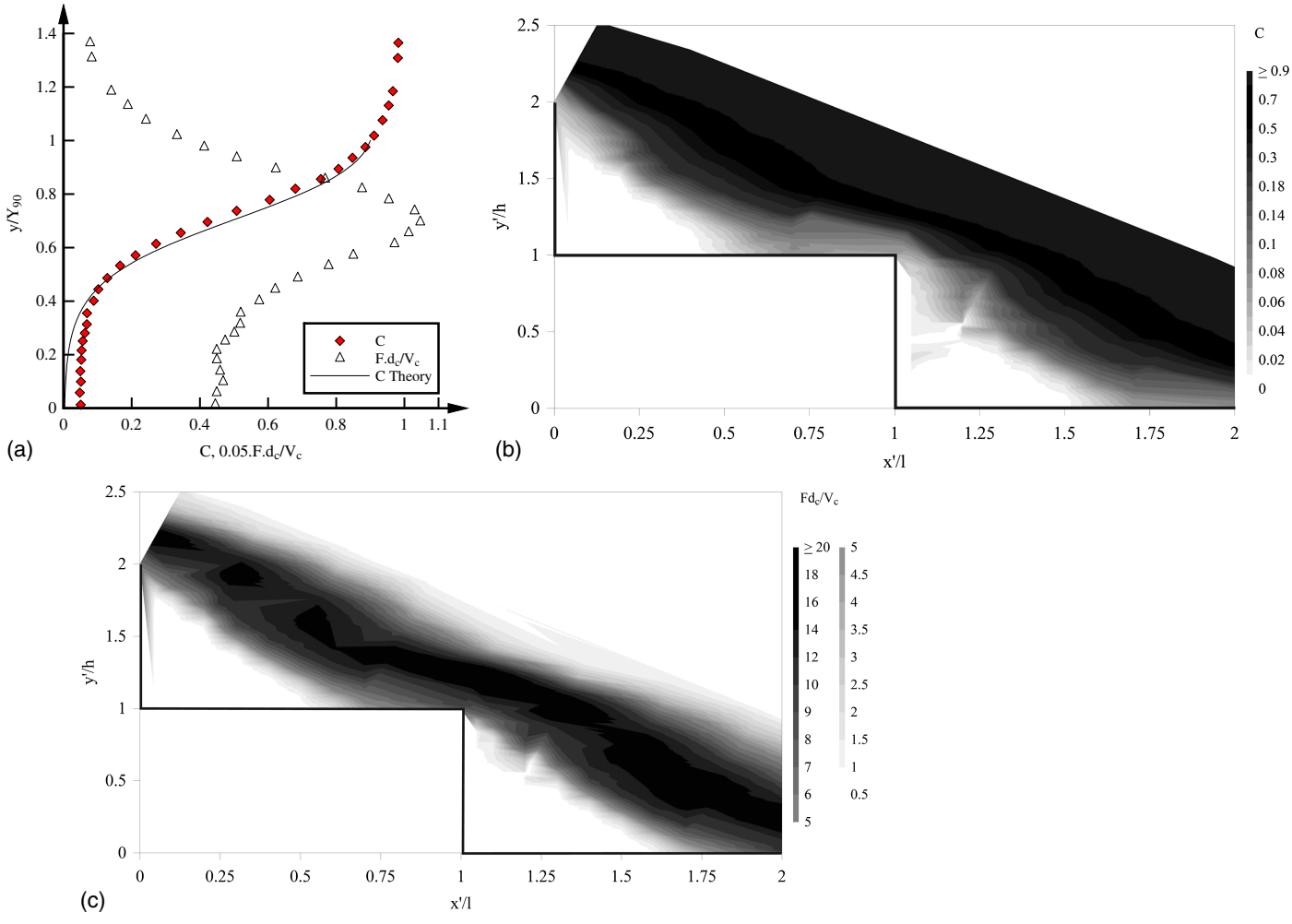

Fig. 2. Void fraction and bubble count rate above gabion stepped chute, including in step cavities: (a) distributions of void fraction and bubble count rate in free-surface flow: $d_c/h = 1.1$, $\mathsf{R} = 4.5 \times 10^5$, step edge 10: comparison between void fraction data and theoretical model of Chanson and Toombes (2002); (b) void fraction contour plot in two consecutive step cavities, $d_c/h = 0.9$, $\mathsf{R} = 3.4 \times 10^5$; (c) dimensionless bubble count rate Fd_c/V_c contour plot in two consecutive step cavities, $d_c/h = 0.9$, $\mathsf{R} = 3.4 \times 10^5$

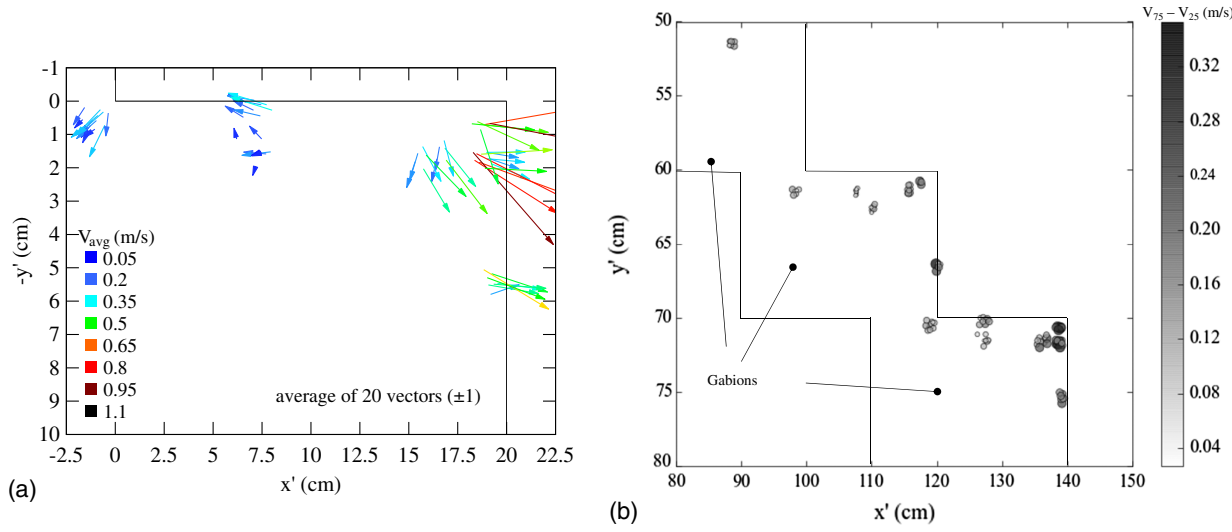

Fig. 3. Bubble velocity measurements in gabions in skimming flow: (a) average bubble velocity vectors at gabion Box 8, $d_c/h = 1.3$, $\mathrm{R} = 5.8 \times 10^5$; (b) bubble velocity fluctuations $(V_{75} - V_{25})$ in gabion Boxes 6–8, $d_c/h = 1.3$, $\mathrm{R} = 5.8 \times 10^5$

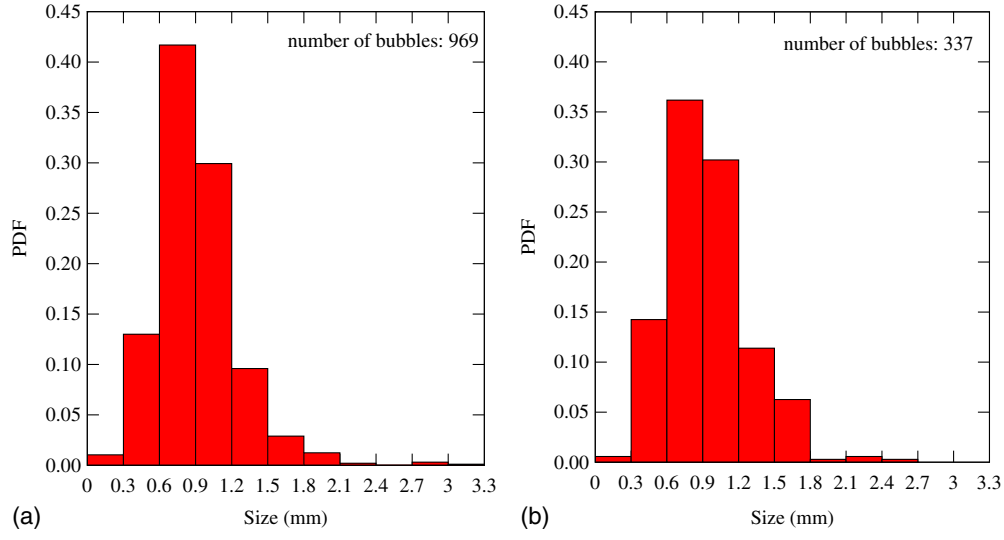

Fig. 4. Bubble size distribution in gabions: (a) left: $d_c/h = 0.7$; (b) right: $d_c/h = 1.3$

Air–Water Flow Properties

Downstream of the inception point of free-surface aeration, free-surface, step-cavity, and seepage flows were highly aerated. At each step edge, the void fraction distributions in skimming free-surface flow presented an inverted S-shape, typical of skimming flows (Chanson and Toombes 2002). An example is shown in Fig. 2(a) including both void fraction and bubble count rate data, where y is the distance normal to the pseudo-bottom (Fig. 1), C is the time-averaged void fraction, F is the bubble count rate, and V_c is the critical flow velocity. Note that the void fraction and bubble count rate were not zero at the step edges ($y = 0$) because of the bubble contents in the gabions [Fig. 2(a)]. In the step cavities beneath the pseudo-bottom ($y < 0$), the void fraction data [Fig. 2(b)] presented a flat shape highlighting the clear water core sketched in Fig. 1. Figs. 2(b and c) present contour plots of void fraction and bubble count rate data, with x' and y' the horizontal and vertical coordinates, respectively, and l the step length: $l = 0.20$ m. The bubble count rate, defined as the number of water-to-air interfaces detected per unit time, gave new information on the interfacial flow structure. In the free-surface flow, the data showed a distinct bubble count rate maximum for local void fractions of approximately 0.4–0.5. In the step cavity, visual observations and phase-detection probe data showed a lesser aeration [Figs. 2(b and c)]. The interfacial velocity data in the free-surface flow presented some self-similar shapes (Zhang and Chanson 2014). In the mainstream, the velocity profiles were close to a power law distribution for $y < Y_{90}$, where Y_{90} is the characteristic elevation where $C = 0.90$. At each step edge, the velocity was not zero at the step edge ($y = 0$) because of the bubble motion in the gabion boxes. Between step edges, the velocity data highlighted a developing shear region in the wake of the step edge (Fig. 1).

The bubbly motion in the gabions was documented with high-speed movies. Typical results are presented in Fig. 3, including the average bubble velocity vectors [Fig. 3(a)] and velocity fluctuations $(V_{75} - V_{25})$, defined as the difference between the third and first

Table 1. Average Air–Water Flow Darcy–Weisbach Friction Factor f_e on Smooth Flat and Gabion Stepped Spillways for $\theta = 26.6°$

Stepped	f_e	
Configuration	Transition flow	Skimming flow
Smooth flat steps	0.174	0.239
Gabion steps	0.080	0.119

Note: Gabion stepped data from Wüthrich and Chanson (2014); present study, smooth flat stepped data from Bung (2009), Felder and Chanson (2011), Guenther et al. (2013), and Wüthrich and Chanson (2014).

quartiles ($V_{75} - V_{25}$), with the symbol sizes proportional to the magnitudes of velocity fluctuations [Fig. 3(c)]. The gabion data showed a high velocity motion in the upper outer corner of each gabion [Fig. 3(a), top right], i.e., maximum mean bubble velocities in excess of 1 m/s and maximum instantaneous velocities of up to 2 m/s. The findings were quantitatively consistent with the interfacial velocity data recorded at $y = 0$ at step edge. Elsewhere in the gabions, the bubble velocities were smaller, but the data showed large velocity fluctuations [Fig. 3(b)]. Inside the gabions, the bubbles presented a variety of shapes and sizes. The characteristic bubble sizes were measured herein perpendicular to the bubble direction. The data indicated some skewed distribution with a preponderance of smaller bubble sizes and a mode of approximately 0.6–0.9 mm (Fig. 4). The observations identified occasional occurrences of large bubbles (>5 mm), mostly inside cavities between large pebbles.

Discussion

The flow resistance was estimated to characterize the combined form and friction losses above the gabion stepped spillway in the air–water flow. An equivalent Darcy–Weisbach friction factor was calculated based on the measured air–water flow properties. The results yielded friction factors between 0.04 and 0.15 (mean value: 0.1). The data were comparable to those of Wüthrich and Chanson (2014). Both gabion spillway data sets are compared to flat smooth stepped spillway data in Table 1, for the same chute slope ($\theta = 26.6°$). The comparison showed a smaller flow resistance on gabion stepped spillways in transition and skimming flow regimes. The gabion stepped chute friction factor was on average half that on smooth flat stepped spillways for the same flow regime and slope. The finding was counterintuitive but likely linked to the effects of exchanges between seepage and recirculation flows. It is proposed that the lower flow resistance resulted from a combination of seepage outflow into the cavity and nonzero velocity at step edges. At each step edge, the overflow velocity was nonzero [$V(y = 0) > 0$], leading to lesser shear stress, compared to smooth flat stepped spillway flows. The gabion seepage outflow into the step cavities further acted as fluid injection into the separated cavity region, reducing the form drag.

Conclusion

On a gabion stepped spillway, both the free-surface and seepage flow motions were investigated. Detailed air–water flow properties were recorded with a phase-detection probe in the free-surface and cavity flows and a high-speed video camera in the gabions. Downstream of the inception point of free-surface aeration, observations indicated a bubbly seepage motion through the gabions with complicated flow patterns and exchanges with the step cavity flow. While the free-surface overflow was highly aerated, the cavity recirculation was, in contrast, less aerated. Bubble tracking in the gabions showed large bubble velocities, particularly next to the step edge. Large bubble velocity fluctuations were recorded throughout the gabions. The gabion stepped spillway friction factor was on average half that on smooth flat stepped spillways for the same conditions. Altogether, the interactions between seepage and free-surface flows were significant, leading to a complex cavity recirculation flow pattern and lesser flow resistance on gabion stepped chutes compared to smooth stepped chutes.

Acknowledgments

The financial support of the Australian Research Council (Grant DP120100481) is acknowledged.

Notation

The following symbols are used in this paper:

C = void fraction;
d_c = critical flow depth (m);
F = bubble count rate (Hz);
f_e = air–water flow Darcy–Weisbach friction factor;
g = gravity acceleration (m/s^2);
h = vertical step height (m);
l = horizontal step length (m);
Q = water discharge (m^3/s);
q = water discharge per unit width (m^2/s);
R = Reynolds number defined in terms of hydraulic diameter;
V = interfacial velocity (m/s);
V_c = critical flow velocity (m/s);
V_{25} = first quartile of velocity data sample (m/s);
V_{75} = third quartile of velocity data sample (m/s);
x = longitudinal coordinate (m);
x' = horizontal coordinate (m);
Y_{90} = characteristic distance (m) where $C = 0.90$;
y = distance (m) normal to pseudo-bottom formed by step edges;
y' = vertical coordinate (m);
θ = angle between pseudo-bottom formed by step edges and horizontal;
ρ = water density (kg/m^3); and
$\emptyset$ = diameter (m).

Subscripts

c = critical flow conditions;
25 = first quartile;
75 = third quartile; and
90 = characteristic air–water flow property for $C = 0.90$.

References

Agostini, R., Bizzarri, A., Masetti, M., and Papetti, A. (1987). "Flexible gabion and Reno mattress structures in river and stream training works. Section one: Weirs." Officine Maccaferri, Bologna, Italy.

Bung, D. B. (2009). "Zur selbstbelüfteten Gerinneströmung auf Kaskaden mit gemäßigter Neigung." Ph.D. dissertation, Bergische Univ. of Wuppertal, Germany.

Chanson, H. (2001). *The hydraulics of stepped chutes and spillways*, Balkema, Lisse, Netherlands.

Chanson, H., and Toombes, L. (2002). "Air-water flows down stepped chutes: Turbulence and flow structure observations." *Int. J. Multiphase Flow*, 28(11), 1737–1761.

Felder, S., and Chanson, H. (2011). "Air-water flow properties in step cavity down a stepped chute." *Int. J. Multiphase Flow*, 37(7), 732–745.

Guenther, P., Felder, S., and Chanson, H. (2013). "Flow aeration, cavity processes and energy dissipation on flat and pooled stepped spillways for embankments." *Environ. Fluid Mech.*, 13(5), 503–525.

Peyras, L., Royet, P., and Degoutte, G. (1992). "Flow and energy dissipation over stepped gabion weirs." *J. Hydraul. Eng.*, 10.1061/(ASCE)0733-9429(1992)118:5(707), 707–717.

Rajaratnam, N. (1990). "Skimming flow in stepped spillways." *J. Hydraul. Eng.*, 10.1061/(ASCE)0733-9429(1990)116:4(587), 587–591.

Sánchez-Juny, M., Bladé, E., and Dolz, J. (2007). "Pressures on a stepped spillway." *J. Hydraul. Res.*, 45(4), 505–511.

Wüthrich, D., and Chanson, H. (2014). "Hydraulics, air entrainment and energy dissipation on gabion stepped weir." *J. Hydraul. Eng.*, 10.1061/(ASCE)HY.1943-7900.0000919, 04014046.

Zhang, G., and Chanson, H. (2014). "Step cavity and Gabion aeration on a Gabion stepped spillway." *Proc., 5th IAHR Int. Symp. on Hydraulic Structures (ISHS2014)*, H. Chanson and L. Toombes, eds., Univ. of Queensland, Brisbane, Australia.